STRUCTURAL STUDY OF SILICA SONOGELS

N. de la ROSA-FOX and L. ESQUIVIAS

Department of Structure and Properties of the Materials, University of Cadiz, Aptdo. 40, Puerto Real (Cadiz), Spain

A.F. CRAIEVICH

Laboratorio Nacional de Luz Sincrotron /CNPq, Campinas, SP and Instituto de Fisica /USP, Sao Paulo, Brazil

J. ZARZYCKI

Laboratory of Science of Vitreous Materials (LA 1119), University of Montpellier II, 34060 Montpellier Cedex, France

Silica sonogels obtained by the hypercritical drying of gels from the hydrolysis of a tetraethoxysilane + water mixture submitted to the action of ultrasounds were studied using small-angle X-ray scattering (SAXS), BET and density measurements. The Guinier regions in SAXS curves are wider and gyration radii are smaller than those of aerogels prepared from alcoholic dilution. These sonogels do not present self-similarity in the accessible scale length of the SAXS measurements. Slopes greater than 4 in the high angle region reveal important electronic density fluctuations on the pore-matrix boundaries, due to their very fine porosity as a consequence of the sonocatalysis.

1. Introduction

One of the reasons for the interest in the research on sol–gel methods from metal alkoxides is that the liquid state allows manipulation at a molecular level. This processing permits a variety of structural modifications, in order to optimize the conditions for the further conversion of the gel into glasses or ceramics.

A classic method of preparation of silica gels is by hydrolysis and polycondensation of $Si(OC_2H_5)_4$ (TEOS) which requires the presence of a solvent (usually ethanol) due to immiscibility of the alkoxide and water. Sonochemistry supplies an additional method for the preparation of silica gels [1], avoiding the use of any solvent, by submitting the alkoxide–water mixture to the action of ultrasounds in the presence of an acid catalyst. It offers a new process to manipulate the molecular aggregation.

Macroscopic parameters indicate important textural differences between aerogels prepared by both methods. It has been shown [2] that aerogels from sonogels are formed from elementary particles smaller than those of 'classic' gels. Sono-

catalysis produces a fine porosity from which gels of high apparent density and surface/volume ratio result. Further, textural parameters appear to be very sensitive to the supplied sonic power and gelation temperature [3,4]. Thus, a higher ultrasonic dose combined with a higher gelling temperature leads to a finer porosity.

Recently, small-angle scattering techniques have been used to test possible fractal features of the aerogels. Thus, according to their aggregation level the gels could show mass fractal [5,6] or else surface fractal features [7]. Although, the boundary between fractal and non-fractal characteristics is still a matter of debate, the scattering data give information about the aggregation levels and geometry of dense systems such as the aerogels studied in this paper.

2. Experimental

2.1. Sample preparation

Sonogels were obtained from hydrolysis and polycondensation of TEOS + H_2O mixtures sub-

jected to the action of ultrasounds [8]. The corresponding classic gels were prepared with a dilution in ethanol.

For sonogel samples SLθ and SHθ designate, respectively, gels prepared at θ °C with either a low ($L \simeq 7$ J cm^{-3}) or high ($H \simeq 15$ J cm^{-3}) dose of ultrasonic energy; above this energy level gelation takes place in situ. In each case TEOS was hydrolyzed with 4 mol H_2O/mol TEOS in acid catalysis (pH $\simeq 1.5$). For classic gels CW–E represents a gel prepared with W mol H_2O/mol TEOS in a solution with E vol. TEOS/vol. ethanol ratio. In all cases the gels were gelled at 50 °C.

The gels were aged for a week and then dried hypercritically [9] under the following autoclave conditions: $P_c = 190$ bar and $T_c = 320$ °C, with a rate of heating of about 4 °C/min. Apparent density d_a was measured by mercury volumetry and the specific surface area S' was measured by the BET method using nitrogen adsorption.

2.2. SAXS measurements

Small-angle X-ray scattering (SAXS) experiments were carried out using the LURE synchrotron radiation facility at Orsay, France. A monochromatized radiation at 8 keV provides a very intense beam with point-like cross-section, using double parallel silicon crystals.

The X-ray beam path was evacuated in order to minimize air scattering. Two photomultipliers placed in front of and behind the sample, perpendicularly to the beam path in a He atmosphere, provide the absorption coefficient of the sample. To record the scattered X-ray intensity a one-dimensional position sensitive detector was used.

To cover a wide range of the scattering vector modulus $q = 4\pi \sin \theta/\lambda$, where θ is the half scattering angle and λ the selected wavelength, two series of data were collected: one series for the detector placed at 30 cm and the other for the detector at 100 cm from the sample.

2.3. SAXS method

Small-angle X-ray scattering gives information about the size and shape distribution of scatterers

as well as other structure-related geometrical parameters. For dense systems the data analysis is subjected to the following restrictions: (a) the system is statistically isotropic and (b) there is no long range order. These conditions permit the assumption that at large r-distance the respective electron densities of each phase become independent [10].

In the low q domain where the Guinier approximation is valid, the data analysis is carried out using the relation

$$I(q) = I(0) \exp\left(-R_G^2 q^2/3\right), \tag{1}$$

where R_G is the radius of gyration which characterizes the distribution of electronic density around the centre of gravity of the particles. For a non-particulate dense system this parameter can be considered as a mean correlation length of the distribution of the matrix solid phase or of the pore phase.

A correlation volume V_c can be defined using the integral $Q_0 = \int_0^\infty I(q)q^2 \, dq$ as a normalizing factor:

$$V_c = 2\pi^2 I(0)/Q_0. \tag{2}$$

For non-particulate systems, V_c can be considered as a geometrical parameter related to the average volume of the heterogeneities.

A first analysis of the SAXS data in the high-q region shows that the product $I(q)q^4$ tends towards a constant which is the expression of Porod's law [10]:

$$\lim_{q \to \infty} \left[I(q)q^4\right] = \frac{Q_0}{\pi \phi_1 \phi_2} \frac{S}{V}, \tag{3}$$

where S/V is the area of the interface per unit volume and ϕ_1, ϕ_2 are the volume fractions of each phase.

A closer analysis of data for this kind of solid revealed positive deviations from Porod's law [11,12] and it should be replaced by the relation

$$\lim\left[I(q)q^4\right] = A + Bq^4. \tag{4}$$

The parameter B is a measure of the deviation from Porod's law, associated with the electronic density fluctuations due to the solid matrix microporosity [13,14]. On the other hand, the parameter A in eq. (4) is related to the surface area of the

matrix–pores interface and strongly depends on surface roughness [15,16].

3. Results and discussions

3.1. Textural characteristics

Using various methods, some textural parameters were measured for comparison with those resulting from SAXS experiments. Thus, from apparent density d_a and specific surface area S', an average pore size can be obtained for use as a reference. These results are shown in table 1; the porous volume V_p was calculated from the skeletal density d_s on a scale of a few ångströms, measured from wide angle X-ray experiments [2] ($d_s = 2.09$ g cm^{-3}).

It can be seen that different modes of formation result in important changes of the textural parameters of gels.

Generally speaking, if the gels contain n_1 micropores with an average size r_1 and n_2 mesopores with an average size r_2, then

$$S'/V_p \propto (n_1/r_1 + n_2/r_2).$$

If the difference between micro- and mesopore size is one order of magnitude, the S'/V_p value is given to a great extent by the number of micropores per unit volume n_1. Thus, for sonogels a greater microporosity can be expected than that for classic gels.
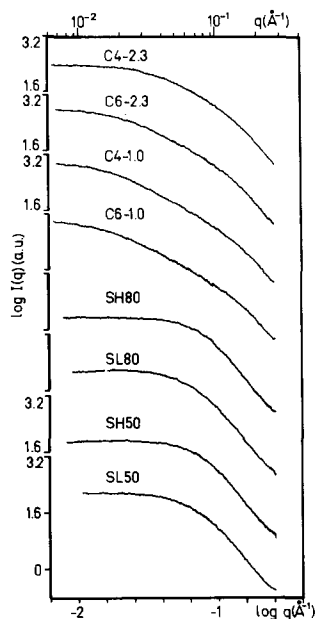

Fig. 1. Log $I(q)$ versus log q for sono- and classic aerogels (for the label of the samples, see section 2.1).

3.2. SAXS analysis

The log $I(q)$ versus log q plots (fig. 1) give information about the homogeneity of the material. Sonogels present a wide plateau in the low q region and, hence, a well defined mean gyration radius, which is characteristic of very homogeneous systems. The point where the curve falls indicates the beginning of the high-q region where the contributions due to structure factor vanish and most scattering corresponds to the particle form factor.

For sonogel samples, the position of this point shifts towards greater q-values with the ultrasonic dose as well as with the gelation temperature. For classic gels, this point is located at smaller q-values. This fact indicates that sonogels are more homogeneous and have a more continuous network on a hundred angstrom length scale.

The curves for the classic gels present an interval in the middle of the q-domain (fig. 1) where a constant slope can be observed but it is doubtful whether the object can be considered as a fractal because the q-region where this linearity is obeyed is very narrow.

Table 1
Textural characteristics of the aerogels

	d_a (g cm^{-3})	S' (m^2 g^{-1})	V_p [a] (cm^3 g^{-1})	$S'/V_p \times 10^{-2}$ (Å^{-1})
SL50	0.65	461	1.06	4.35
SL80	0.65	370	1.06	3.45
SH50	0.82	407	0.74	5.56
SH80	0.83	387	0.73	5.26
C6–1.0	0.31	646	2.75	2.33
C4–1.0	0.38	517	2.15	2.38
C6–2.3	0.39	612	2.09	2.94
C4–2.3	0.53	545	1.41	3.85

[a] $V_p = 1/d_a - 1/d_s$.

3.2.1. Average correlation radius (R_G)

A linear fit of the ln $I(q)$ versus q^2 in the low-q domain permits a determination of the average correlation radius as well as, by extrapolation, the zero angle intensity $I(0)$ (eq. 1). The linear regions are more extended in the q-domain for the sonogels and present smaller R_G values than those for classic gels. These results are summarized in table 2.

R' represents the mean correlation radius if we assume that the correlation volume V_c has a spherical geometry. It can be seen, for sonogels, that these R'-values are in agreement with this geometry. However, for classic gels, there is an important deviation due to surface shape. These results should be related to the boundary surface roughness between solid matrix–empty pores. Thus, the sonogels show a smoother surface probably due to the action of cavitation bubbles in the first stages of the condensation process. This surface can be considered as a consequence of a pregelation stage on the surface of the cavitation bubbles, hence their spherical shape. Afterwards the condensation starts linking these particles into a low density solid matrix.

3.2.2. Skeletal density

The positive deviation of the $I(q)q^4$ function in the asymptotic q range is more important for sonogels than for classic gels, as can be seen in fig. 2. In order to calculate the value of $\phi(1-\phi)$ from eq. (3), plots of $I(q)q^4$ versus q^4 have been drawn in order to determine the fluctuation parameter B of eq. (4). From these curves and
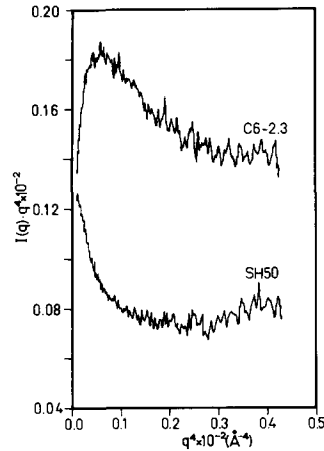

Fig. 2. Porod plots for sonogel SH50 (with high ultrasonic dose and gelled at 50°C) and classic gel C6–2.3 (with $W = 6$ and 70 vol.% TEOS in ethanol).

using eq. (3), the $\phi(1-\phi)$ value has been determined for all samples. Most of the values of $\phi(1-\phi)$ are higher than 0.25. This suggests that the two-levels electronic density model does not apply here and that a more complex model, involving at least a three-level electronic density, should be considered.

4. Conclusion

Small-angle X-ray scattering intensities measurements from silica aerogels reveal the possibility of analyzing the characteristics of dense systems built of non-particulate aggregates. The results reveal various structures of the aerogels which are a function of their mode of formation.

For classic aerogels the structure consists of a low density matrix with large empty pores and with an extremely rough but sharp interface. The matrix does not present density fluctuations and therefore no deviation from Porod's law is observed for these gels. However, the structures show only a narrow self-similarity range on the length scale accessible to SAXS experiments and cannot be considered as fractal objects.

On the other hand, the sonogels have a finer porosity. The pores are approximately spherical-shaped indicating a smooth surface. The wide

Table 2
SAXS parameters for aerogels from experimental intensities

	$I(0)$ (a.u.)	$Q_0 \times 10^{-2}$ (Å^{-3})	R_G (Å)	R' (Å)
SL50	167.34	2.63	28	24
SL80	169.02	2.35	29	25
SH50	99.48	2.07	25	22
SH80	100.48	2.17	25	22
C6–1.0	1042.42	3.02	89	42
C4–1.0	976.63	2.95	82	42
C6–2.3	613.57	3.05	63	35
C4–2.3	232.53	2.89	39	26

Guinier region shows a high uniformity in the distribution of the aggregates. The matrix presents electron density fluctuations in all cases, that can be due to the mode of formation specific to sono-catalysis.

The impossibility of determining the skeletal density of most of the studied samples by using the classical SAXS method implies that the two-electronic density model, even including density fluctuations, is not satisfactory for describing the structure of dense sono- and classic aerogels.

References

[1] M. Tarasevich, Am. Ceram. Bull. 63 (1984) 500.
[2] L. Esquivias, C. Barrera-Solano, N. de la Rosa-Fox, F.L. Cumbrera and J. Zarzycki, in: Proc. 4th Int. Conf on Ultrastructure Processing of Glasses and Composites, Tucson, AZ (1989) eds. D.R. Uhlmann and D.R. Ulrich (Wiley, New York, 1990) in press.
[3] N. de La Rosa-Fox, L. Esquivias and J. Zarzycki, Diff. Defect Data 53–54 (1987) 363.
[4] N. de la Rosa-Fox, L. Esquivias and J. Zarzycki, Rev. Phys. Appl., Colloq. C4 24 (1989) C4-233.
[5] M.A. Aegerter, D.I. dos Santos, A.F. Craievich, T. Lours and J. Zarzycki, Diff. Defect Data 53–54 (1987) 427.
[6] D.I. dos Santos, M.A. Aegerter, A.F. Craievich, T. Lours and J. Zarzycki, J. Non-Cryst. Solids 95–96 (1987) 1143.
[7] D.W. Schaefer, Science 243 (1989) 1023.
[8] L. Esquivias and J. Zarzycki, in: Current Topics on Non-Crystalline Solids, eds. M.D. Baro and N. Clavaguera (World Scientific, Singapore, 1986) p. 409.
[9] J. Zarzycki, M. Prassas and J. Phalippou, J. Mater. Sci. 17 (1982) 3371.
[10] G. Porod, in: Small Angle X-Ray Scattering, eds. O. Glatter and O. Kratky (Academic Press, London, 1982) p. 17.
[11] W. Ruland, J. Appl. Cryst. 4 (1971) 70.
[12] J.T. Koberstein, B. Morra and R.S. Stein, J. Appl. Cryst. 13 (1980) 34.
[13] I. Strawbridge, A.F. Craievich and P.F. James, J. Non-Cryst. Solids 72 (1985) 139.
[14] A.F. Craievich, J. Appl. Cryst. 20 (1987) 327.
[15] A.J. Hurd, D.W. Schaefer and A.M. Glines, J. Appl. Cryst. 21 (1988) 864.
[16] K.D. Keefer and D.W. Schaefer, Phys. Rev. Lett. 56 (1986) 2376.